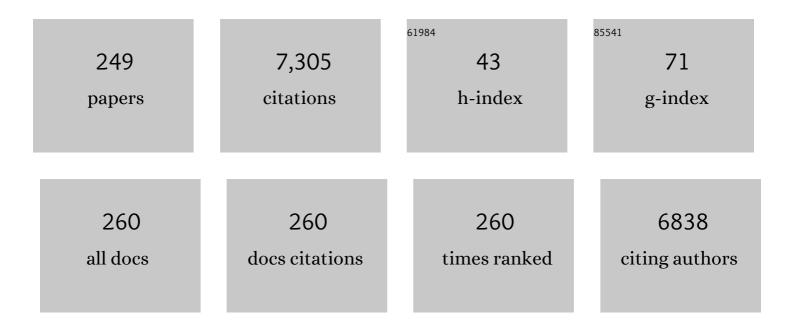
Gilberto Artioli

List of Publications by Year in descending order

Source: https://exaly.com/author-pdf/6555728/publications.pdf Version: 2024-02-01



#	Article	IF	CITATIONS
1	Archaeological assessment reveals Earth's early transformation through land use. Science, 2019, 365, 897-902.	12.6	369
2	The nature of disorder in montmorillonite by simulation of X-ray powder patterns. American Mineralogist, 2002, 87, 966-975.	1.9	258
3	Ti Location in the MFI Framework of Tiâ^'Silicalite-1:Â A Neutron Powder Diffraction Study. Journal of the American Chemical Society, 2001, 123, 2204-2212.	13.7	190
4	Pressure-Induced Volume Expansion of Zeolites in the Natrolite Family. Journal of the American Chemical Society, 2002, 124, 5466-5475.	13.7	188
5	Kinetic study of the kaolinite-mullite reaction sequence. Part I: Kaolinite dehydroxylation. Physics and Chemistry of Minerals, 1995, 22, 207.	0.8	179
6	Recommended nomenclature for zeolite minerals: report of the subcommittee on zeolites of the International Mineralogical Association, Commission on New Minerals and Mineral Names. Mineralogical Magazine, 1998, 62, 533-571.	1.4	157
7	Segregation Vesicles, Gas Filter-Pressing, and Igneous Differentiation. Journal of Geology, 1984, 92, 55-72.	1.4	152
8	High-Pressure Raman Spectroscopic Study of Spinel (ZnCr2O4). Journal of Solid State Chemistry, 2002, 165, 165-170.	2.9	130
9	Kinetic study of the kaolinite-mullite reaction sequence. Part II: Mullite formation. Physics and Chemistry of Minerals, 1995, 22, 215.	0.8	119
10	Structural Characterization of Ti-Silicalite-1: A Synchrotron Radiation X-Ray Powder Diffraction Study. Journal of Catalysis, 1999, 183, 222-231.	6.2	117
11	Neutron powder diffraction study of orthorhombic and monoclinic defective silicalite. Acta Crystallographica Section B: Structural Science, 2000, 56, 2-10.	1.8	110
12	Characterisation of defective silicalites â€. Dalton Transactions RSC, 2000, , 3921-3929.	2.3	108
13	Crystal structure of AlPO4-21, a framework aluminophosphate containing tetrahedral phosphorus and both tetrahedral and trigonal-bipyramidal aluminum in 3-, 4-, 5-, and 8-rings. Inorganic Chemistry, 1985, 24, 188-193.	4.0	102
14	Chemical analyses of Bronze Age glasses from Frattesina di Rovigo, Northern Italy. Journal of Archaeological Science, 2004, 31, 1175-1184.	2.4	96
15	Negative thermal expansion and local dynamics inCu2OandAg2O. Physical Review B, 2006, 73, .	3.2	95
16	Kinetics of formation of zeolite Na-A [LTA] from natural kaolinites. Physics and Chemistry of Minerals, 1997, 24, 191-199.	0.8	94
17	Octahedral cation ordering in olivine at high temperature. II: an in situ neutron powder diffraction study on synthetic MgFeSiO 4 (Fa50). Physics and Chemistry of Minerals, 2000, 27, 630-637.	0.8	87
18	High temperature dehydroxylation of muscovite-2M 1 : a kinetic study by in situ XRPD. Physics and Chemistry of Minerals, 1999, 26, 375-381.	0.8	84

#	Article	IF	CITATIONS
19	Multipurpose imaging-plate camera forin situpowder XRD at the GILDA beamline. Journal of Synchrotron Radiation, 2001, 8, 1162-1166.	2.4	81
20	Kinetic study of the dehydroxylation of chrysotile asbestos with temperature by in situ XRPD. Physics and Chemistry of Minerals, 2003, 30, 177-183.	0.8	81
21	Template Burning inside TS-1 and Fe-MFI Molecular Sieves:Â An in Situ XRPD Study. Journal of the American Chemical Society, 2003, 125, 14549-14558.	13.7	79
22	Thermal expansion in cuprite-type structures from 10â€K to decomposition temperature: Cu2O and Ag2O. Journal of Applied Crystallography, 2003, 36, 1461-1463.	4.5	73
23	Recommended nomenclature for zeolite minerals: Report of the Subcommittee on Zeolites of the International Mineralogical Association, Commission on New Minerals and Mineral Names. European Journal of Mineralogy, 1998, 10, 1037-1081.	1.3	72
24	X-ray diffraction microtomography (XRD-CT), a novel tool for non-invasive mapping of phase development in cement materials. Analytical and Bioanalytical Chemistry, 2010, 397, 2131-2136.	3.7	71
25	On the Crystal Structure and Cation Valence of Mn in Mn-Substituted Ba-β-Al2O3. Journal of Catalysis, 1998, 179, 597-605.	6.2	70
26	Orthorhombic to monoclinic phase transition in high-Ti-loaded TS-1: an attempt to locate Ti in the MFI framework by low temperature XRD. Microporous and Mesoporous Materials, 2000, 40, 85-94.	4.4	70
27	First Structural Investigation of a Super-Hydrated Zeolite. Journal of the American Chemical Society, 2001, 123, 12732-12733.	13.7	67
28	Tricalcium aluminate hydration in additivated systems. A crystallographic study by SR-XRPD. Cement and Concrete Research, 2008, 38, 477-486.	11.0	66
29	A universal curve of apatite crystallinity for the assessment of bone integrity and preservation. Scientific Reports, 2018, 8, 12025.	3.3	66
30	A lead-isotope database of copper ores from the Southeastern Alps: A tool for the investigation of prehistoric copper metallurgy. Journal of Archaeological Science, 2016, 75, 27-39.	2.4	65
31	Crystal structure-crystal chemistry relationships in the zeolites erionite and offretite. American Mineralogist, 1998, 83, 590-606.	1.9	63
32	X-ray single-crystal diffraction study of pyrope in the temperature range 30-973 K. American Mineralogist, 1995, 80, 457-464.	1.9	61
33	Dehydration dynamics of stilbite using synchrotron X-ray powder diffraction. American Mineralogist, 1997, 82, 729-739.	1.9	59
34	Stabilization of lead contaminated soil with traditional and alternative binders. Journal of Hazardous Materials, 2020, 382, 120990.	12.4	59
35	LIA of Prehistoric Metals in the Central Mediterranean Area: A Review. Archaeometry, 2020, 62, 53-85.	1.3	57
36	Crystal structure of coesite, a high-pressure form of silica, at 15 and 298 K from single-crystal neutron and x-ray diffraction data: test of bonding models. The Journal of Physical Chemistry, 1987, 91, 988-992.	2.9	53

#	Article	lF	CITATIONS
37	Nature of Structural Disorder in Natural Kaolinites: A New Model Based on Computer Simulation of Powder Diffraction Data and Electrostatic Energy Calculation. Clays and Clay Minerals, 1995, 43, 438-445.	1.3	53
38	Crystals and phase transitions in protohistoric glass materials. Phase Transitions, 2008, 81, 233-252.	1.3	53
39	Bone diagenesis at the micro-scale: Bone alteration patterns during multiple burial phases at Al Khiday (Khartoum, Sudan) between the Early Holocene and the II century AD. Palaeogeography, Palaeoclimatology, Palaeoecology, 2014, 416, 30-42.	2.3	53
40	Bone diagenesis variability among multiple burial phases at Al Khiday (Sudan) investigated by ATR-FTIR spectroscopy. Palaeogeography, Palaeoclimatology, Palaeoecology, 2016, 463, 168-179.	2.3	52
41	Kinetics of nucleation and growth of zeolite LTA from clear solution by in situ and ex situ XRPD. Microporous and Mesoporous Materials, 2002, 54, 105-112.	4.4	51
42	Crystal chemistry of the zeolites erionite and offretite. American Mineralogist, 1998, 83, 577-589.	1.9	48
43	The Crystal Structures of Orthorhombic and Monoclinic Palygorskite. Materials Science Forum, 1994, 166-169, 647-652.	0.3	45
44	Discriminating pottery production by image analysis: a case study of Mesolithic and Neolithic pottery from Al Khiday (Khartoum, Sudan). Journal of Archaeological Science, 2014, 46, 125-143.	2.4	45
45	The dehydration process in the zeolite laumontite: a real-time synchrotron X-ray powder diffraction study. Physics and Chemistry of Minerals, 1996, 23, 328.	0.8	44
46	Preparation and Dating of Mortar Samples—Mortar Dating Inter-Comparison Study (MODIS). Radiocarbon, 2017, 59, 1845-1858.	1.8	44
47	Synchrotron X-ray Rietveld study of perlialite, the natural counterpart of synthetic zeolite-L. European Journal of Mineralogy, 1990, 2, 749-760.	1.3	44
48	Cellular glass–ceramics from a self foaming mixture of glass and basalt scoria. Journal of Non-Crystalline Solids, 2014, 403, 38-46.	3.1	42
49	Cement hydration: the role of adsorption and crystal growth. Crystal Research and Technology, 2013, 48, 903-918.	1.3	41
50	Late Bronze Age Copper Smelting Slags from Luserna (Trentino, Italy): Interpretation of the Metallurgical Process. Archaeometry, 2016, 58, 96-114.	1.3	39
51	Mortar Dating Methodology: Assessing Recurrent Issues and Needs for Further Research. Radiocarbon, 2017, 59, 1859-1871.	1.8	39
52	Neutron diffraction study of natrolite, Na2Al2Si3O10.2H2O, at 20 K. Acta Crystallographica Section C: Crystal Structure Communications, 1984, 40, 1658-1662.	0.4	37
53	XAFS characterization of the structural site of Yb in synthetic pyrope and grossular garnets. Physics and Chemistry of Minerals, 1999, 26, 251-256.	0.8	37
54	Crystallographic texture analysis of archaeological metals: interpretation of manufacturing techniques. Applied Physics A: Materials Science and Processing, 2007, 89, 899-908.	2.3	37

#	Article	IF	CITATIONS
55	Evidence of calcium carbonates in coastal (Talos Dome and Ross Sea area) East Antarctica snow and firn: Environmental and climatic implications. Earth and Planetary Science Letters, 2008, 271, 43-52.	4.4	37
56	In the footsteps of Pliny: tracing the sources of Garamantian carnelian from Fazzan, south-west Libya. Journal of Archaeological Science, 2014, 52, 218-241.	2.4	37
57	Shall we abandon sedimentation methods for particle size analysis in soils?. Soil and Tillage Research, 2019, 185, 36-46.	5.6	37
58	Lead isotope systematics in hydrothermal sulphide deposits from the central-eastern Southalpine (northern Italy). European Journal of Mineralogy, 2012, 24, 23-37.	1.3	36
59	Eneolithic copper smelting slags in the Eastern Alps: Local patterns of metallurgical exploitation in the Copper Age. Journal of Archaeological Science, 2015, 63, 78-83.	2.4	36
60	Long-distance connections in the Copper Age: New evidence from the Alpine Iceman's copper axe. PLoS ONE, 2017, 12, e0179263.	2.5	36
61	The thermal behaviour of cuprite: An XRD–EXAFS combined approach. Nuclear Instruments & Methods in Physics Research B, 2003, 200, 231-236.	1.4	35
62	Thermal expansion and phase transitions in åkermanite and gehlenite. Physics and Chemistry of Minerals, 2005, 32, 189-196.	0.8	35
63	Neutron diffraction structure refinement of the zeolite gismondine at 15 K. Zeolites, 1986, 6, 361-366.	0.5	34
64	Kinetic study of hydroxysodalite formation from natural kaolinites by time-resolved synchrotron powder diffraction. Microporous Materials, 1997, 9, 189-201.	1.6	33
65	Examining microstructural evolution of Portland cements by in-situ synchrotron micro-tomography. Journal of Materials Science, 2015, 50, 1805-1817.	3.7	33
66	Kinetic Model of Calcium-Silicate Hydrate Nucleation and Growth in the Presence of PCE Superplasticizers. Crystal Growth and Design, 2016, 16, 646-654.	3.0	33
67	Single-crystal neutron diffraction study of partially dehydrated laumontite at 15 K. Zeolites, 1989, 9, 377-391.	0.5	32
68	Fully hydrated laumontite: A structure study by flat-plate and capillary powder diffraction techniques. Zeolites, 1993, 13, 249-255.	0.5	32
69	High-temperature behaviour of melilite: in situ X-ray diffraction study of gehlenite–åkermanite–Na melilite solid solution. Physics and Chemistry of Minerals, 2008, 35, 147-155.	0.8	32
70	Thermal expansion and stability of Ti2SC in air and inert atmospheres. Journal of Alloys and Compounds, 2009, 469, 395-400.	5.5	32
71	Understanding cement hydration at the microscale: new opportunities from `pencil-beam' synchrotron X-ray diffraction tomography. Journal of Applied Crystallography, 2013, 46, 142-152.	4.5	31
72	Selecting the Most Reliable ¹⁴ C Dating Material Inside Mortars: the Origin of the Padua Cathedral. Radiocarbon, 2019, 61, 375-393.	1.8	31

#	Article	IF	CITATIONS
73	Neutron diffraction study of the zeolite yugawaralite at 13 K*. Zeitschrift Für Kristallographie, 1986, 174, 265-281.	1.1	30
74	Gonnardite; re-examination of holotype material and discreditation of tetranatrolite. American Mineralogist, 1999, 84, 1445-1450.	1.9	30
75	Octahedral cation ordering in olivine at high temperature. I: in situ neutron single-crystal diffraction studies on natural mantle olivines (Fa12 and Fa10). Physics and Chemistry of Minerals, 2000, 27, 623-629.	0.8	30
76	Secondary phosphates in the ceramic materials from Frattesina (Rovigo, North-Eastern Italy). Journal of Cultural Heritage, 2009, 10, 144-151.	3.3	30
77	<i>Inâ€Situ</i> XRD Measurement and Quantitative Analysis of Hydrating Cement: Implications for Sulfate Incorporation in C–S–H. Journal of the American Ceramic Society, 2015, 98, 1259-1264.	3.8	29
78	Cement-stabilized contaminated soil: Understanding Pb retention with XANES and Raman spectroscopy. Science of the Total Environment, 2021, 752, 141826.	8.0	29
79	Microscopic strain in synthetic pyrope-grossular solid solutions determined by synchrotron X-ray powder diffraction at 5 K: The relationship to enthalpy of mixing behavior. American Mineralogist, 2005, 90, 506-509.	1.9	28
80	Towards three-dimensional quantitative reconstruction of cement microstructure by X-ray diffraction microtomography. Journal of Applied Crystallography, 2011, 44, 272-280.	4.5	28
81	Direct Imaging of Nucleation Mechanisms by Synchrotron Diffraction Micro-Tomography: Superplasticizer-Induced Change of C–S–H Nucleation in Cement. Crystal Growth and Design, 2015, 15, 20-23.	3.0	27
82	The State-of-the-Art of Dating Techniques Applied to Ancient Mortars and Binders: A Review. Radiocarbon, 2020, 62, 503-525.	1.8	27
83	In situ powder neutron diffraction of cation partitioning vs. pressure in Mg (sub 0.94) Al (sub 2.04) O ₄ synthetic spinel. American Mineralogist, 1999, 84, 905-912.	1.9	26
84	The early hydration and the set of Portland cements: <i>In situ</i> X-ray powder diffraction studies. Powder Diffraction, 2007, 22, 201-208.	0.2	26
85	Simulation of the hydration kinetics and elastic moduli of cement mortars by microstructural modelling. Cement and Concrete Composites, 2014, 52, 54-63.	10.7	26
86	Moving metals IV: Swords, metal sources and trade networks in Bronze Age Europe. Journal of Archaeological Science: Reports, 2019, 26, 101837.	0.5	26
87	X-ray structure refinement of mesolite. Acta Crystallographica Section C: Crystal Structure Communications, 1986, 42, 937-942.	0.4	25
88	Synthesis and characterization of white micas in the join muscovite–aluminoceladonite. American Mineralogist, 2001, 86, 555-565.	1.9	25
89	Non-ideality and defectivity of the akermanite-gehlenite solid solution: An X-ray diffraction and TEM study. American Mineralogist, 2007, 92, 1685-1694.	1.9	25
90	A neutron powder diffraction study of fully deuterated laumontite. European Journal of Mineralogy, 1993. 5. 851-856.	1.3	25

#	Article	IF	CITATIONS
91	Diagenetic mordenite from Ponza, Italy. European Journal of Mineralogy, 1995, 7, 429-438.	1.3	25
92	Dispersion relations of acoustic phonons in pyrope garnet; relationship between vibrational properties and elastic constants. American Mineralogist, 1996, 81, 19-25.	1.9	24
93	Negative thermal expansion in cuprite-type compounds: A combined synchrotron XRPD, EXAFS, and computational study of Cu2O and Ag2O. Journal of Physics and Chemistry of Solids, 2006, 67, 1918-1922.	4.0	24
94	Mineralogical clustering of the structural mortars from the Sarno Baths, Pompeii: A tool to interpret construction techniques and relative chronologies. Journal of Cultural Heritage, 2019, 40, 265-273.	3.3	24
95	A Fresh View on Limestone Calcined Clay Cement (LC3) Pastes. Materials, 2021, 14, 3037.	2.9	24
96	Single-crystal pulsed neutron diffraction of a highly hydrous beryl. Acta Crystallographica Section B: Structural Science, 1995, 51, 733-737.	1.8	23
97	Multifractal Analysis of Calcium Silicate Hydrate (<scp><scp>C</scp>–<scp>scp>S</scp>–<scp>S</scp>–<scp>H</scp></scp>) Mapped by <scp>X</scp> â€ray Diffraction Microtomography. Journal of the American Ceramic Society, 2012, 95, 2647-2652.	3.8	23
98	Crystal chemistry of cement-asbestos. American Mineralogist, 2013, 98, 1095-1105.	1.9	23
99	The effect of oxidation and reduction on thermal expansion of magnetite from 298 to 1173K at different vacuum conditions. Journal of Solid State Chemistry, 2004, 177, 1713-1716.	2.9	22
100	Raman hyperspectral imaging as an effective and highly informative tool to study the diagenetic alteration of fossil bones. Talanta, 2018, 179, 167-176.	5.5	22
101	XANES study of titanium coordination in natural diopsidic pyroxenes. European Journal of Mineralogy, 1993, 5, 1101-1110.	1.3	22
102	Highâ€Temperature Thermal Expansion and Stability of V ₂ AlC Up To 950°C. Journal of the American Ceramic Society, 2007, 90, 3013-3016.	3.8	21
103	The crystal structure of Mg8(Mg2Al2)Al8Si12(O,OH)56pumpellyite and its relevance in ultramafic systems at high pressure. American Mineralogist, 1999, 84, 1906-1914.	1.9	20
104	Imaging of nano-seeded nucleation in cement pastes by X-ray diffraction tomography. International Journal of Materials Research, 2014, 105, 628-631.	0.3	20
105	The pigments of the frigidarium in the Sarno Baths, Pompeii: Identification, stratigraphy and weathering. Journal of Cultural Heritage, 2019, 40, 309-316.	3.3	20
106	Pseudotachylyte Alteration and the Rapid Fade of Earthquake Scars From the Geological Record. Geophysical Research Letters, 2020, 47, e2020GL090020.	4.0	20
107	The Vitruvian legacy: Mortars and binders before and after the Roman world. , 2019, , 151-202.		20
108	The crystal chemistry of pumpellyite: An X-ray Rietveld refinement and 57Fe M�ssbauer study. Physics and Chemistry of Minerals, 1994, 20, 443.	0.8	19

#	Article	IF	CITATIONS
109	Microstructure imaging of C54–TiSi2 polycrystalline thin films by micro-Raman spectroscopy. Applied Physics Letters, 1999, 75, 3090-3092.	3.3	19
110	In situ dehydration of yugawaralite. American Mineralogist, 2001, 86, 185-192.	1.9	19
111	Technological transfers in the Mediterranean on the verge of Romanization: Insights from the waterproofing renders of Nora (Sardinia, Italy). Journal of Cultural Heritage, 2020, 44, 63-82.	3.3	18
112	Inelastic neutron scattering from pyrope powder: experimental data and theoretical calculations. European Journal of Mineralogy, 1998, 10, 59-70.	1.3	18
113	Mn crystal chemistry in pumpellyite; a resonant scattering powder diffraction Rietveld study using synchrotron radiation. American Mineralogist, 1996, 81, 603-610.	1.9	17
114	Crystal chemistry, cation ordering and thermoelastic behaviour of CoMgSiO4 olivine at high temperature as studied by in situ neutron powder diffraction. Physics and Chemistry of Minerals, 2005, 32, 655-664.	0.8	17
115	Neutrons in cultural heritage research. Journal of Neutron Research, 2006, 14, 37-42.	1.1	17
116	Science for the cultural heritage: the contribution of X-ray diffraction. Rendiconti Lincei, 2013, 24, 55-62.	2.2	17
117	Lime-based injection grouts with reduced water content: An assessment of the effects of the water-reducing agents ovalbumin and ethanol on the mineralogical evolution and properties of grouts. Journal of Cultural Heritage, 2018, 30, 70-80.	3.3	17
118	MgAl2O4 synthetic spinel: cation and vacancy distribution as a function of temperature, from in situ neutron powder diffraction. Zeitschrift Fur Kristallographie - Crystalline Materials, 2000, 215, 406-412.	0.8	16
119	The crystal chemistry of julgoldite-Fe3+from Bombay, India, studied using synchrotron X-ray powder diffraction and57Fe Mössbauer spectroscopy. American Mineralogist, 2003, 88, 1084-1090.	1.9	16
120	High temperature structural and thermoelastic behaviour of mantle orthopyroxene: an in situ neutron powder diffraction study. Physics and Chemistry of Minerals, 2007, 34, 185-200.	0.8	16
121	Mineralogy and archaeometry: fatal attraction. European Journal of Mineralogy, 2011, 23, 849-855.	1.3	16
122	Role of fruit flesh cell morphology and MdPG1 allelotype in influencing juiciness and texture properties in apple. Postharvest Biology and Technology, 2020, 164, 111161.	6.0	16
123	The Elusive Crystal Structure of Uric Acid Dihydrate: Implication for Epitaxial Growth During Biomineralization. Acta Crystallographica Section B: Structural Science, 1997, 53, 498-503.	1.8	15
124	High temperature reactions in mold flux slags: Kinetic versus composition control. Journal of Non-Crystalline Solids, 2007, 353, 2852-2860.	3.1	15
125	Use of nanocomposites as permeability reducing admixtures. Journal of the American Ceramic Society, 2018, 101, 4275-4284.	3.8	15
126	The Evolution of the Vitruvian Recipes over 500 Years of Floorâ€Making Techniques: The Case Studies of the <i>Domus delle Bestie Ferite</i> and the <i>Domus di Tito Macro</i> (Aquileia, Italy). Archaeometry, 2018, 60, 185-206.	1.3	15

#	Article	IF	CITATIONS
127	Calcium aluminate cement as an alternative to ordinary Portland cement for the remediation of heavy metals contaminated soil: mechanisms and performance. Journal of Soils and Sediments, 2021, 21, 1755-1768.	3.0	15
128	Gobbinsite from Magheramorne Quarry, Northern Ireland. Mineralogical Magazine, 1994, 58, 615-620.	1.4	15
129	Retention of phosphorus and fluorine in phosphogypsum for cemented paste backfill: Experimental and numerical simulation studies. Environmental Research, 2022, 214, 113775.	7.5	15
130	Synthetic phosphorus-substituted analcime, Na13Al24Si13P11O96.16H2O with ordered Al and Si/P. Acta Crystallographica Section C: Crystal Structure Communications, 1984, 40, 214-217.	0.4	14
131	Cation partitioning versus temperature in (Mg 0.70 Fe 0.23)Al 1.97 O 4 synthetic spinel by in situ neutron powder diffraction. Physics and Chemistry of Minerals, 1999, 26, 242-250.	0.8	14
132	In situsimultaneous synchrotron powder diffraction and mass spectrometry study of methane anaerobic combustion on iron-oxide-based oxygen carrier. Journal of Applied Crystallography, 2005, 38, 353-360.	4.5	14
133	Improving the performance of PCE superplasticizers in early stiffening Portland cement. Construction and Building Materials, 2017, 130, 83-91.	7.2	14
134	Radiocarbon dating reveals the timing of formation and development of pedogenic calcium carbonate concretions in Central Sudan during the Holocene. Geochimica Et Cosmochimica Acta, 2018, 238, 16-35.	3.9	14
135	The Cannero Castle (Italy): Development of Radiocarbon Dating Methodologies in the Framework of the Layered Double Hydroxide Mortars. Radiocarbon, 2020, 62, 617-631.	1.8	14
136	X-ray absorption study at the Fe K-edge of garnets from the Ivrea-Verbano zone. Mineralogical Magazine, 1993, 57, 249-255.	1.4	14
137	Vingt ans de recherches à Saint-Véran, Hautes Alpes: état des connaissances de l'activité de production de cuivre à l'âge du Bronze ancien. Trabajos De Prehistoria, 2010, 67, 269-285.	¹ 0.7	14
138	Chemical and mineralogical studies on hominid remains from Sangiran, Central Java (Indonesia). Journal of Human Evolution, 1993, 24, 57-68.	2.6	13
139	On the space group of garronite. Powder Diffraction, 1999, 14, 190-194.	0.2	13
140	Growth morphology of gypsum in the presence of copolymers. Crystal Research and Technology, 2011, 46, 1010-1018.	1.3	13
141	Neutron diffraction of Cu–Zn–Sn ternary alloys: non-invasive assessment of the compositions of historical bronze/brass copper ternary alloys. Journal of Applied Crystallography, 2017, 50, 49-60.	4.5	13
142	NEARCHOS. Networked Archaeological Open Science: Advances in Archaeology Through Field Analytics and Scientific Community Sharing. Journal of Archaeological Research, 2018, 26, 447-469.	4.0	13
143	Copper to Tuscany – Coals to Newcastle? The dynamics of metalwork exchange in early Italy. PLoS ONE, 2020, 15, e0227259.	2.5	13
144	Characterization of the Natural Zeolite Gonnardite. Structure Analysis of Natural and Cation Exchanged Species by the Rietveld Method. Materials Science Forum, 1991, 79-82, 845-850.	0.3	12

#	Article	IF	CITATIONS
145	Single-crystal neutron diffraction. European Journal of Mineralogy, 2002, 14, 233-239.	1.3	12
146	A temperature dependent X-ray Absorption Fine Structure study of dynamic X-site disorder in almandine: a comparison to diffraction data. Physics and Chemistry of Minerals, 1997, 24, 200-205.	0.8	11
147	Thermal Expansion of Chromites and Zinc Spinels. Materials Science Forum, 1998, 278-281, 390-395.	0.3	11
148	Study of the negative thermal expansion of cuprite-type structures by means of temperature-dependent pair distribution function analysis: Preliminary results. Journal of Physics and Chemistry of Solids, 2008, 69, 2182-2186.	4.0	11
149	GAMBLING WITH ETRUSCAN DICE: A TALE OF NUMBERS AND LETTERS. Archaeometry, 2011, 53, 1031-1043.	1.3	11
150	3D imaging of complex materials: the case of cement. International Journal of Materials Research, 2012, 103, 145-150.	0.3	11
151	5. Role of hydrotalcite-type layered double hydroxides in delayed pozzolanic reactions and their bearing on mortar dating. , 2017, , 147-158.		11
152	Combining multispectral images with X-ray fluorescence to quantify the distribution of pigments in the frigidarium of the Sarno Baths, Pompeii. Journal of Cultural Heritage, 2019, 40, 317-323.	3.3	11
153	Prescreening Hydraulic Lime-Binders for Disordered Calcite in Caesarea Maritima: Characterizing the Chemical Environment Using FTIR. Radiocarbon, 2020, 62, 527-543.	1.8	11
154	Molecular H2O in armenite, BaCa2Al6Si9O30·2H2O, and epididymite, Na2Be2Si6O15·H2O: Heat capacity, entropy and local-bonding behavior of confined H2O in microporous silicates. Geochimica Et Cosmochimica Acta, 2010, 74, 5202-5215.	3.9	10
155	Late Bronze Age copper smelting in the southeastern Alps: how standardized was the smelting process? Evidence from Transacqua and Segonzano, Trentino, Italy. Archaeological and Anthropological Sciences, 2017, 9, 985-999.	1.8	10
156	Lattice parameters determination from powder diffraction data: Results from a round robin project. Powder Diffraction, 1996, 11, 253-258.	0.2	9
157	Site Differentiation by Synchrotron Radiation Resonant Scattering:Â Case Study of BaZn2Ge2. Chemistry of Materials, 1997, 9, 1463-1466.	6.7	9
158	In situ powder diffraction studies of temperature induced transformations in minerals. Nuclear Instruments & Methods in Physics Research B, 1997, 133, 45-49.	1.4	9
159	Quantitative Phase Analysis of Natural Raw Materials Containing Montmorillonite. Materials Science Forum, 2001, 378-381, 702-709.	0.3	9
160	Molecular resolution images of the surfaces of natural zeolites by atomic force microscopy. Microporous and Mesoporous Materials, 2003, 61, 79-84.	4.4	9
161	Lead isotope systematics in ophiolite-associated sulphide deposits from the Western Alps and Northern Apennine (Italy). European Journal of Mineralogy, 2018, 30, 17-31.	1.3	9
162	Metal flow in the late Bronze Age across the Friuli-Venezia Giulia plain (Italy): new insights on Cervignano and Muscoli hoards by chemical and isotopic investigations. Archaeological and Anthropological Sciences, 2019, 11, 4829-4846.	1.8	9

#	Article	IF	CITATIONS
163	Late Pleistocene/Early Holocene Evidence of Prostatic Stones at Al Khiday Cemetery, Central Sudan. PLoS ONE, 2017, 12, e0169524.	2.5	9
164	An Atomistic Model Describing the Structure and Morphology of Cu-Doped C-S-H Hardening Accelerator Nanoparticles. Nanomaterials, 2022, 12, 342.	4.1	9
165	Highâ€performing mortarâ€based materials from the late imperial baths of Aquileia: An outstanding example of Roman building tradition in Northern Italy. Geoarchaeology - an International Journal, 2022, 37, 637-657.	1.5	9
166	Multiple hydrogen positions in the zeolite brewsterite, (Sr0.95,Ba0.05)Al2Si6O16.5H2O. Acta Crystallographica Section C: Crystal Structure Communications, 1985, 41, 492-497.	0.4	8
167	Profile-Fitting Treatment of Single-Crystal Diffraction Data. Acta Crystallographica Section A: Foundations and Advances, 1996, 52, 890-897.	0.3	8
168	The Dehydration Process in the Natural Zeolite Laumontite: A Real-Time Synchrotron X-Ray Powder Diffraction Study. Materials Science Forum, 1996, 228-231, 369-374.	0.3	8
169	Chromium crystal chemistry mullite–spinel refractory ceramics. Materials Research Bulletin, 1999, 34, 711-720.	5.2	8
170	Role of Phosphate Species and Speciation Kinetics in Detergency Solutions. Industrial & Engineering Chemistry Research, 2012, 51, 4173-4180.	3.7	8
171	Consecutive thermal and wet conditioning treatments of sedimentary stabilized cementitious materials from HPSS® technology: Effects on leaching and microstructure. Journal of Environmental Management, 2019, 250, 109503.	7.8	8
172	Low temperature SR-XRPD study of åkermanite-gehlenite solid solution. Zeitschrift Für Kristallographie, Supplement, 2006, 2006, 419-424.	0.5	8
173	Integrated multi-analytical screening approach for reliable radiocarbon dating of ancient mortars. Scientific Reports, 2022, 12, 3339.	3.3	8
174	The crystal chemistry of cowlesite. Mineralogical Magazine, 1992, 56, 575-579.	1.4	7
175	New milarite/osumilite-type phase formed during ancient glazing of an Egyptian scarab. Applied Physics A: Materials Science and Processing, 2013, 110, 371-377.	2.3	7
176	Provenancing ancient pigments: Lead isotope analyses of the copper compound of egyptian blue pigments from ancient mediterranean artefacts. Journal of Archaeological Science: Reports, 2017, 16, 1-18.	0.5	7
177	Differentiating between long and short range disorder in infra-red spectra: on the meaning of "crystallinity―in silica. Physical Chemistry Chemical Physics, 2017, 19, 21783-21790.	2.8	7
178	Salt pans as a new archaeological sea-level proxy: A test case from Dalmatia, Croatia. Quaternary Science Reviews, 2020, 250, 106680.	3.0	7
179	Dehydroxylation Kinetics of Muscovite-2M ₁ . Materials Science Forum, 1998, 278-281, 424-429.	0.3	6
180	The mystery of the discolored flints. New molecules turn prehistoric lithic artifacts blue. Analytical and Bioanalytical Chemistry, 2011, 399, 2389-2393.	3.7	6

#	Article	IF	CITATIONS
181	Synchrotron radiation XRPD study on the early hydration of cements. Zeitschrift Für Kristallographie, Supplement, 2007, 2007, 411-416.	0.5	6
182	High-temperature <i>in situ</i> Rietveld study of Fe,Mg cation partitioning in olivine. Powder Diffraction, 1994, 9, 63-67.	0.2	5
183	In situ dynamic light scattering and synchrotron X-ray powder diffraction study of the early stages of zeolite growth. Studies in Surface Science and Catalysis, 2002, , 45-52.	1.5	5
184	THE BLUE ENAMELS IN THE BAROQUE DECORATIONS OF THE CHURCHES OF PALERMO, SICILY: FE2+-COLOURED GLASSES FROM LIME KILNS. Archaeometry, 2009, 51, 197-213.	1.3	5
185	Morphological reconstruction of Roman arrowheads from Iulia Concordia: Italy. Applied Physics A: Materials Science and Processing, 2014, 117, 1227-1240.	2.3	5
186	Non-invasive assessment of the formation of tourmaline nodules by X-ray microtomography and computer modeling. American Mineralogist, 2015, 100, 459-465.	1.9	5
187	The Contribution of Geoscience to Cultural Heritage Studies. Elements, 2016, 12, 13-18.	0.5	5
188	The silver treasure of Marengo: silver provenancing and insights into late antiquity Roman and Gallo-Roman hoards. Archaeological and Anthropological Sciences, 2019, 11, 4959-4970.	1.8	5
189	Probing the provenance of archaeological glaze colorants: Polychrome faunal reliefs of the Ishtar Gate and the Processional Way of Babylon. Archaeometry, 2019, 61, 837-855.	1.3	5
190	Ochre-Based Pigments in the Tablinum of the House of the Bicentenary (Herculaneum, Italy) between Decorative Technology and Natural Disasters. Minerals (Basel, Switzerland), 2021, 11, 67.	2.0	5
191	Evaluation of the phase detection limit on filter-deposited dust particles from Antarctic ice cores. Zeitschrift Für Kristallographie, Supplement, 2007, 2007, 73-78.	0.5	5
192	Phasing the history of ancient buildings through PCA on mortars' mineralogical profiles: the example of the Sarno Baths (Pompeii). Archaeometry, 2022, 64, 866-882.	1.3	5
193	High Temperature Phase Transition of Muscovite-2 <i>M</i> ₁ : Angle and Energy Dispersive Powder Diffraction Studies. Materials Science Forum, 1994, 166-169, 547-552.	0.3	4
194	Low-Ca pyroxenes from LL group chondritic meteorites: crystal structural studies and implications for their thermal histories. Earth and Planetary Science Letters, 1994, 128, 469-478.	4.4	4
195	The grid-work texture of authigenic microcrystalline quartz in siliceous crust-type (SCT) mineralized horizons. American Mineralogist, 2002, 87, 1128-1138.	1.9	4
196	Residual strain mapping of Roman styli from Iulia Concordia, Italy. Materials Characterization, 2014, 91, 58-64.	4.4	4
197	Mineralogical interpretation of multispectral images: The case study of the pigments in the frigidarium of the Sarno Baths, Pompeii. Journal of Archaeological Science: Reports, 2021, 35, 102774.	0.5	4
198	57Fe-Mössbauer investigation on garnets from the Ivrea-Verbano Zone. Mineralogical Magazine, 1993, 57, 671-676.	1.4	4

#	Article	IF	CITATIONS
199	Glass and other vitreous materials through history. , 2019, , 87-150.		4
200	Thermal Expansion of C ₃ S and Mg-Doped Alite. Materials Science Forum, 1998, 278-281, 384-389.	0.3	3
201	Thermal Expansion and Excess Properties of Ãkermanite-Gehlenite Synthetic Solid Solution Series. Materials Science Forum, 2004, 443-444, 401-406.	0.3	3
202	In situ waxs-saxs synchrotron study of the kinetics of nucleation and growth in linde type-a zeolite (LTA). Studies in Surface Science and Catalysis, 2004, 154, 355-363.	1.5	3
203	EXAFS and XRD Study of Local Dynamics in Cu2O and Ag2O. Physica Scripta, 2005, , 271.	2.5	3
204	Structural characterisation of high-temperature K-exchanged sodalite. Zeitschrift Für Kristallographie, Supplement, 2006, 2006, 437-442.	0.5	3
205	Mineralogy and Cultural Heritage. Chimia, 2010, 64, 712-715.	0.6	3
206	On the preparation of concentrated gypsum slurry to reuse sulfate-process TiO2 byproduct stream. Journal of Cleaner Production, 2018, 195, 1468-1475.	9.3	3
207	Foreword: The MACH Project and the case study of the Sarno Baths in Pompeii. Journal of Cultural Heritage, 2019, 40, 228.	3.3	3
208	An Anatolian-Style Lead Figurine from the Assyrian Colony Period Found in the Middle Bronze Age Palace of Tel Kabri. Bulletin of the American Schools of Oriental Research, 2021, 385, 87-97.	0.2	3
209	The crystal structure of a new calcium aluminate phase containing formate. Cement and Concrete Research, 2021, 146, 106490.	11.0	3
210	Chemical, Mineralogical and Textural Characterisation of Early Iron Age Vitreous Materials from the Golasecca Culture (Northern Italy). , 2011, , 25-32.		3
211	Crystal chemistry of clinker relicts from aged cementitious materials. Journal of Applied Crystallography, 2014, 47, 1626-1637.	4.5	3
212	Microtopographic features and dissolution behavior of natural zeolite surfaces studied by Atomic Force Microscopy (AFM). Studies in Surface Science and Catalysis, 2002, 142, 1721-1728.	1.5	2
213	Local lattice dynamics and negative thermal expansion in crystals. Journal of Physics: Conference Series, 2007, 92, 012153.	0.4	2
214	Improving the quality of 63Cu/65Cu ratio determination by ICP-QMS through a careful evaluation of instrumental performances. Journal of Analytical Atomic Spectrometry, 2010, 25, 893.	3.0	2
215	The dissolution of laumontite in acidic aqueous solutions: A controlled-temperature in situ atomic force microscopy study. American Mineralogist, 2012, 97, 150-158.	1.9	2

216 Modern and ancient masonry: Nature and role of the binder. , 2016, , 3-10.

2

#	Article	IF	CITATIONS
217	Morphological reconstruction of Roman styli from Iulia Concordia—Italy. Archaeological and Anthropological Sciences, 2018, 10, 781-794.	1.8	2
218	Nanoseeds as modifiers of the cement hydration kinetics. , 2020, , 257-269.		2
219	Unusual Luminescence of Quartz from La Sassa, Tuscany: Insights on the Crystal and Defect Nanostructure of Quartz. Minerals (Basel, Switzerland), 2021, 11, 1345.	2.0	2
220	A multitechnique approach for the identification of multiple contamination sources near a polluted industrial site. Land Degradation and Development, 2022, 33, 2317-2326.	3.9	2
221	Neutron Diffraction Studies of the Hydrogen Bonding and Water Molecules in Zeolites. Studies in Surface Science and Catalysis, 1985, , 249-254.	1.5	1
222	Packing analysis of racket-like molecules: C6H5MX (M=metal, X=Cl, Br, I). Crystal structure determination of microcrystalline C6H5HgCl by XRD. Journal of Crystallographic and Spectroscopic Research, 1993, 23, 595-600.	0.2	1
223	Inorganic Compounds and Minerals Studied Using X-Ray Diffraction*. , 1999, , 1048-1056.		1
224	surface reactivity of minerals. European Journal of Mineralogy, 2007, 19, 295-295.	1.3	1
225	Role of Polycarboxylate-ether superplasticizers on cement hydration kinetics and microstructural development. MATEC Web of Conferences, 2018, 149, 01004.	0.2	1
226	Temperature Dependence of Disorder and Correlation Effets in the Almandine X-Site. European Physical Journal Special Topics, 1997, 7, C2-1157-C2-1158.	0.2	1
227	Powder Diffraction and Synchrotron Radiation. , 2015, , 319-336.		1
228	Introduction: The role of modern mineralogy in cultural heritage studies. , 2019, , 1-12.		1
229	Gaming in Pre-Roman Italy: Characterization of Early Ligurian and Etruscan Small Pieces, Including Dice. Applied Sciences (Switzerland), 2022, 12, 2130.	2.5	1
230	Cation Partitioning in Mg _{0.70} Fe _{0.23} Al _{1.97} O _{4Synthetic Spinels by <i> in situ</i> Neutron Powder Diffraction. Materials Science Forum, 1998, 278-281, 692-697.}	08gt;	0
231	Synchrotron X-Ray Powder Diffraction Study of (Bi,Pb)1.64Sr1.43Ca1.57Mn2O9, Mn-Analogue of BSCCO-2212 Superconductor. Journal of Solid State Chemistry, 1999, 147, 501-508.	2.9	0
232	SPECIAL ISSUE . THE LINKING ROLE OF THE ALPS IN PAST CULTURES: AN ARCHAEOMETRIC APPROACH. Archaeometry, 2005, 47, i-ii.	1.3	0
233	X-Ray Diffraction, Studies of Inorganic Compounds and Minerals. , 2017, , 676-683.		0

Powder diffraction in art and archaeology. , 2019, , 759-766.

#	Article	IF	CITATIONS
235	Study of the Initial Stage of Zeolite A Synthesis by Dynamic Light Scattering and Synchrotron X-Ray Diffraction. , 2000, , .		0
236	Ti sites in TS-1: recent data and evidence. Acta Crystallographica Section A: Foundations and Advances, 2002, 58, c41-c41.	0.3	0
237	In situsynchrotron XRD studies of combustion processes. Acta Crystallographica Section A: Foundations and Advances, 2005, 61, c87-c87.	0.3	0
238	Simultaneous XRPD-MS study on iron oxides supported on spinel-like aluminate. Acta Crystallographica Section A: Foundations and Advances, 2005, 61, c140-c140.	0.3	0
239	Combined XRPD and spectroscopic study of molecules hosted in zeolitic channels. Acta Crystallographica Section A: Foundations and Advances, 2005, 61, c40-c40.	0.3	0
240	Structural characterisation of hightemperature K-exchanged sodalite. , 2006, , 437-442.		0
241	Low temperature SR-XRPD study of $ ilde{A}$ kermanite-gehlenite solid solution. , 2006, , 419-424.		0
242	A synchrotron diffraction study of microscopic strain in garnet solid solutions. Acta Crystallographica Section A: Foundations and Advances, 2007, 63, s100-s100.	0.3	0
243	Studies of the synthesis and transformation of materials usingin situtime-resolved powder diffraction. Acta Crystallographica Section A: Foundations and Advances, 1996, 52, C22-C23.	0.3	0
244	In Situ Structural and Kinetic Powder Diffraction Studies of Aluminosilicates. , 1999, , 177-187.		0
245	X-ray Diffraction (XRD). Encyclopedia of Earth Sciences Series, 2017, , 1019-1025.	0.1	0
246	Role of Polycarboxylate-ether superplasticizers on cement hydration kinetics and microstructural development. MATEC Web of Conferences, 2018, 149, 01004.	0.2	0
247	Water molecules in natural zeolites studied by neutron diffraction. Acta Crystallographica Section A: Foundations and Advances, 1984, 40, C375-C375.	0.3	0
248	Innovative Calcium Carbonate-Based Products to Repair Cracked Cement Mortars. Materials, 2022, 15, 4044.	2.9	0
249	Unusual Luminescence of Quartz from La Sassa, Tuscany: Insights on the Crystal and Defect Nanostructure of Quartz Further Developments. Minerals (Basel, Switzerland), 2022, 12, 828.	2.0	0